Hybrid Metal Foams

Mechanical Testing and Determination of Mass Flow Limitations During Electroplating

Anne Jung [*1], Michael R. Koblischka[2], Erhardt Lach[4], Stefan Diebels[1], Harald Natter[3]

[1]Department of Applied Mechanics, Saarland University, 66123 Saarbruecken, Germany

[2]Department of Experimental Physics, Saarland University, 66123 Saarbruecken, Germany

[3]Department of Physical Chemistry, Saarland University, 66123 Saarbruecken, Germany

[4]French German Research Institute of Saint-Louis, 68300 Saint-Louis, France

[*1]anne.jung@mx.uni-saarland.de;

Abstract

Electrodeposition is a non-line of sight deposition technique which is also applicable for complex 3D structures. Even with this outstanding coating method there is a challenge in electroplating of complex 3D materials with a high porosity. In this work we developed special process parameter regarding the design of the plating cell and deposition parameter to ensure a nearly homogeneous coating of open cell metal foams. Based on field scans of the magnetic flux density a technique for the determination of the coating thickness distribution of magnetic coatings in a foam has been developed. The deposition process and thus the coating thickness distribution of porous 3D cathodes strongly depends on mass transport limitations. Two qualitative models to describe the mass transport limitations for direct current plating and pulsed electrodeposition can be deduced of the field scans of the magnetic flux density. X-ray computed tomography shows hydrogen evolution as a further coating-problem. Quasi-static compressions tests have been performed on nickel and copper coated foams, respectively. The coating metal has a significant effect on the mechanical properties of such a hybrid foam consisting of a coating on an aluminium substrate foam.

Keywords

Electrodeposition; Metal Foams; Nanocrystalline; Magnetic Flux Density; Compression Tests

Introduction

Metal foams are a very interesting class of biomimetric structures. They are highly porous cellular metals with a 3D open network of pores and mimic the construction elements of bones, wood or cork [1]-[2]. According to this spectacular mesoscopic structure, this structuring shows a high stiffness-to-weight ratio and an excellent energy absorption capacity. Open cell metal foams especially based on aluminium became of significant interest for applications in aerospace, automotive and mechanical engineering [3]-[4]. For these fields of application they are used as lightweight construction elements, energy absorber or for structural damping. Further applications are filters, heat exchangers and catalyst supports [3]-[5].

Based on the open porous structure of metal foams, they can be used as cathode in electroplating processes for reinforcement of lightweight aluminium foams. Only a few works [6]-[7] are known about this topic. These works describe the coating of very thin foams with a thickness of less than 12 mm. The general problem is the ratio of the coating thickness of the outer struts and the centre is about 2 which means, there is a highly inhomogeneity of the coating thickness distribution over the foam cross section. As shown by Euler [8] the deposition process and hence the thickness of the coating in porous electrodes are strongly influenced by mass transport limitation. A deeper understanding of this mass transport limitation is necessary to improve the homogeneity of the coating thickness distribution. Coating of metal foams can improve the mechanical properties or provide additional functions like corrosion resistance or catalytic activities. The excellent mechanical properties (stiffness and energy absorption) of a hybrid foam based on an aluminium foam with a nanocrystalline nickel coating have been shown in a previous work [9]. In this work we developed a qualitative model to describe the degree of inhomogeneity of the coating thickness distribution by measuring the magnetic flux density distribution of nickel coated foams. With these results it was possible to improve the coating process and to adopt to other coating metals like copper.

Materials and Methods

Plating Procedure

Electrodeposition is a versatile and common non-line

of sight technique for the preparation of metals and alloys [10]-[12]. In his study aluminum foams (AlSi7Mg0.3 by m-pore, Dresden, Germany) with pore size of 10 ppi (pores per inch), were plated by direct current (DC) or pulsed electrodeposition (PED) with nanocrystalline nickel.

Before the electrodeposition an 8 steps pre-treatment (pickling and electroless deposition) is necessary to protect the aluminum based foams from dissolution in the acid electrolyte. The pickling does although improve the adhesion of the coating. The pretreatment process is outlined in Fig. 1.
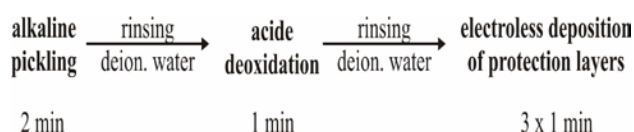

FIG. 1 PRE-TREATMENT OF THE ALUMINUM FOAMS

All steps were carried out at room temperature with rinsing in deion. water after each step. A commercial nickel sulfamate electrolyte with 110 g/L nickel (Enthone, GmbH, Langenfeld, Germany) was used at 50°C and a pH of 3.8. For the copper coating a copper sulfate electrolyte has been used (200 g/L $CuSO_4 \times 4H_2O$, 50 g/L H_2SO_4, 0.2 g/L surfactant, 40°C, pH = 1). The exact plating parameters are mentioned for each experiment.

In contrast to planar electrodes the plating of 3D porous materials requires a special anode-cathode configuration. The anode consists of a double-walled hollow cube, built of expanded titanium metal and filled with nickel pieces (Ni, A.M.P.E.R.E. GmbH, Dietzenbach, Germany) or even copper tubes as sacrificial anode. The cathode consists of an aluminum foam, placed in the centre of the cage-like anode. The depositions were carried out in a thermostated electrolysis cell with a volume of 3500 ml.

Mass Transport Limitation

Coating of such complex three dimensional electrodes causes a special mass transport limitation. In the case of DC-plating there are two concentration zones in front of a planar bulk electrode. The first zone is the bulk electrolyte; with a constant concentration of the metal ions. In the second zone between the cathode and the bulk electrolyte consists of a linear metal ion gradient. At the limiting diffusion current the concentration at the cathode surface is zero [13]. Open-cell metal foams are substantially more complex three-dimensional electrodes. The above mentioned

concentration profile for planar electrodes has to be expanded into a third dimension. During the electrodeposition of foams each of the struts can act as a planar electrode as described above. The problem is outlined in Fig. 2. It describes an open cell metal foam plunged into an electrolyte. If no current is applied, the metal ions are homogeneously distributed over the cross-section of the foam. After applying a current, all metal ions within and in the vicinity of the foam will be spontaneously deposited. To continue the coating process, metal ions have to diffuse from the bulk of the electrolyte to the centre of the foam.

Based on the fact, that there is a deposition of metal ions all way from the outer regions of the metal foam to the centre of the foam, only a few ions will reach the centre of the foam. In the inner of the foam occurs an ion diffusion due to a gradient in the ion concentration. This mass transport limitation by diffusion during the plating process causes a non-uniform coating thickness distribution on the struts. A second effect which let to a certain inhomogeneity of the coating is the electromagnetic shielding from outer ligaments of the foam which acts as a faraday cage [6].
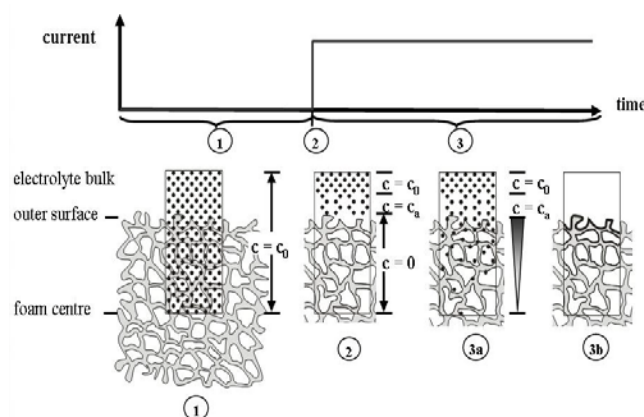

FIG. 2 SCHEME OF THE METAL IONS DISTRIBUTION IN THE FOAM DURING DIRECT CURRENT PLATING (DC). (1) ZERO CURRENT, (2) APPLIED CURRENT: DEPLETION OF METAL-IONS IN THE CENTRE OF THE FOAM (3A) DIFFUSION OF METAL IONS FROM THE BULK ELECTROLYTE INTO THE FOAM, (3B) INHOMOGENEOUS COATING THICKNESS DISTRIBUTION DUE TO MASS TRANSPORT LIMITATION

In contrast to planar electrodes the plating of 3D porous materials requires a special anode-cathode configuration. The anode consists of a double-walled hollow cube, built of expanded titanium.

Pulsed electrodeposition should produce a more homogeneous coating thickness distribution than DC plating. Fig. 3 shows a scheme of the distribution of metal ions in a foam during the pulsed
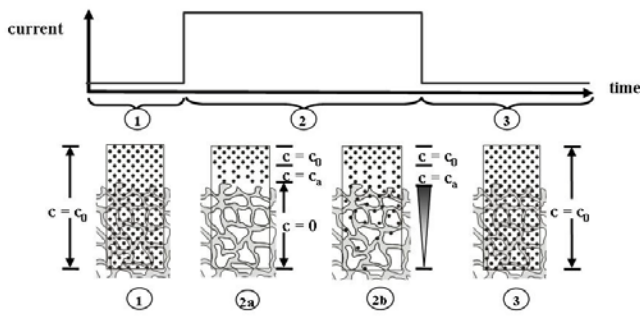
electrodeposition process.

FIG. 3 SCHEME OF THE METAL IONS DISTRIBUTION IN THE FOAM DURING PULSED ELECTRODEPOSITION (PED). (1) ZERO CURRENT (T_{OFF}-TIME) (2) CURRENT PULSE (T_{ON}-TIME), (2A) DEPLETION OF THE METAL-IONS IN THE FOAM, (2B) DIFFUSION OF METAL IONS FROM THE ELECTROLYTE BULK INTO THE FOAM CENTRE AND DEPOSITION, (3) T_{OFF} TIME: THE METAL IONS ARE ABLE TO DIFFUSE TO THE FOAM CENTRE WITHOUT DEPOSITION

Similar to the direct current plating process, the metal ions in the vicinity of the foam surface will be spontaneously deposited during the t_{on}-time. There is the depletion of the electrolyte in the pores. In the following t_{off}-time the metal ions diffuse from the electrolyte bulk to the foam centre without deposition at the outer ligaments of the foam. Increasing t_{off}-times should improve the homogeneity of the coating thickness distribution.

Characterization

Scanning of the Magnetic Flux Density

A method to visualize the coating thickness distribution of a coated foam sample is a prerequisite for the enhancement of the homogeneity of the coating thickness by optimizing the plating parameters. For ferromagnetic coatings like nickel, we developed a method to visualize the metal distribution by scanning of the magnetic flux density distribution in analogy to the trapped field scans performed now routinely on bulk high-Tc superconductors [14]-[16]; Christides et al. were also applying this technique to bulk permanent magnets [17]. The coated aluminum foam cubes are cut into several rectangular plates. The plates are introduced into a Helmholtz coil with a homogeneous magnetic field of 256 mT oriented perpendicular to the longest axis of the foam pieces to force a defined initial magnetic state on the foam plates. The metal distribution of each foam plate is determined by measuring the remnant magnetic flux density distribution Bz(x,y) by scanning the surface of the foam with a commercial Hall probe (Arepoc, Bratislava, Slovakia; magnetic resolution 0.1 G) in a

fixed distance of 1.5 mm above the sample surface. Fig. 4 shows the five measuring planes (MP) of a foam sample which was cut into four plates. The measuring setup for the field scan of nickel-coated metal foams is also displayed.
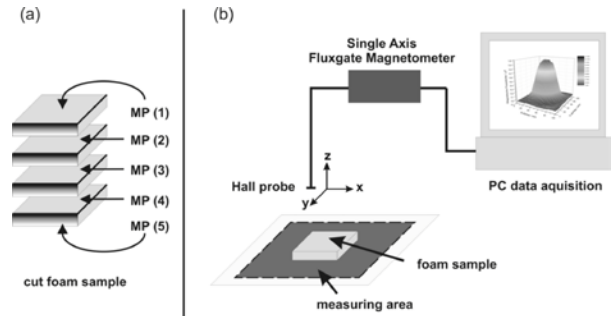

FIG. 4 (A) THE MEASURING PLANES OF A FOAM SAMPLE AND (B) SCHEMATIC DRAWING OF THE MEASURING SETUP

A Hall probe fixed on a x-y-z-stage is able to scan in a distance of 15 mm above the foam plates. The dimensions of the measuring area were the three-fold of the dimensions of the foam in x- and y-direction. The information about the thickness distribution and its spatial distribution results from the measured trapped field. Additional information about this method supplied for coated metal foams can be found in a previous work [18].

Characterization of the Nanostructure

The crystallite size, crystallite size distribution and microstrain of the nanostructured metallic coatings have been determined by X-ray diffraction (XRD; Siemens D500, Bruker AXS, Germany) using a modified Warren-Averbach method [19]-[21]. The nickel coatings of all samples have a crystallite size of 43 nm ± 2 nm. A characterization of the morphology of the foam substrates and coatings has been carried out using scanning electron microscopy (SEM; Jeol JSM 7000 F). To have a closer look on the homogeneity and quality of the coating thickness over the foam and the structure of the foam, X-ray computed tomography (Fraunhofer IZFP, Saarbrücken, Germany) has been performed on coated and uncoated aluminum foams.

SEM and X-ray Computed Tomography

The surface morphologies of the uncoated aluminum foams and a nickel coating are shown in Fig. 5. The uncoated aluminum foams have a rough surface built of bumps. The nickel coating has a smoother surface morphology. Round bumps which are close to each other built a fully covering coating. This cauliflower-like structuring results from a radial grain growth process resulting from a hemispherical ion diffusion.

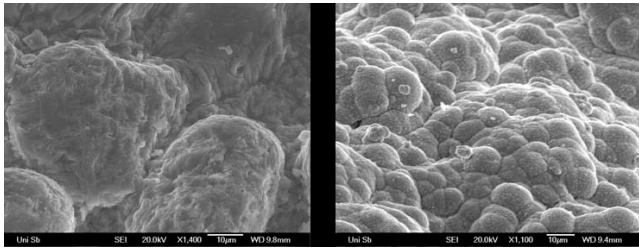This structure increases the specific surface area of a foam.

FIG. 5 SEM-IMAGES OF AN UNCOATED ALUMINUM FOAM (X1400, LEFT) AND THE DC NI COATING (X1100, RIGHT)

Fig. 6 shows X-ray computed tomograms of an uncoated aluminum foam and a nickel coated foam with a coating thickness of 150 μm (deposited at a DC current density of 1.1 mA/cm²). The tomogram outlines an almost homogeneous coating thickness distribution for the cross-section of the foam. Due to the side reaction of hydrogen evolution, the coating contains some pinhole defects caused by the sticking hydrogen. To avoid the embrittlement of the coating by grain refiners, we do not use any surfactants.
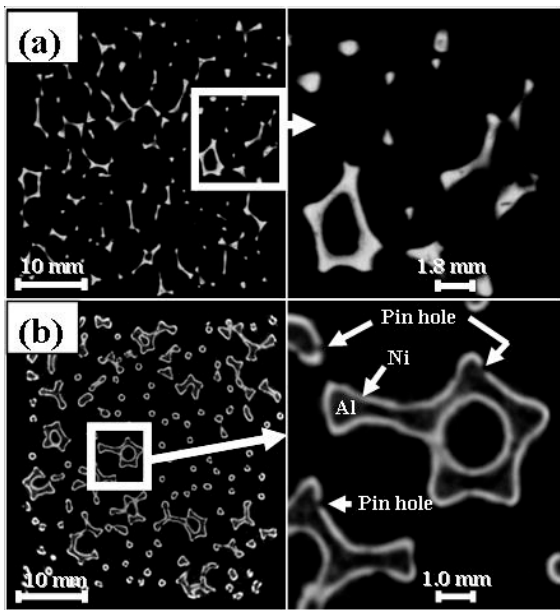

FIG. 6 X-RAY COMPUTED TOMOGRAMS OF AN UNCOATED ALUMINUM FOAM (A) AND A NICKEL COATED ALUMINUM FOAM WITH A COATING THICKNESS OF 150 μM

Quasi-static Compression Tests

In order to investigate the effect of different coating metals and coating thicknesses, cubic 10 ppi aluminium foams with an edge length of 40 mm have been coated with nickel and copper, respectively. The theoretical coating thicknesses vary in 50 μm steps between 0 and 250 μm for each coating metal. The hybrid foams have been tested on an INSTRON universal testing machine under compressive loading at strain rates of about $5 \cdot 10^{-3}$ s^{-1}. According to the very complexe structure of the metal foams, there is a common significant scattering in the results. Based on this fact and for a better statistics, each sample type has been tested at least three times.

Results and Discussion

Field Scans of the Magnetic Flux Density

In order to optimize the applied average current density for DC nickel plating, cubic 10 ppi foams (40 x 40 x 40 mm³) were coated at different current densities. The theoretical all-over coating thickness should be 20 μm. After the plating process each foam was cut into rectangular plates with a thickness of 10 mm. Trapped field scans of the magnetic flux density, B_z, were performed on each of these foam cuts. Maximal relative flux densities results for four plates of foam samples coated at different applied current densities are shown in Fig. 7.
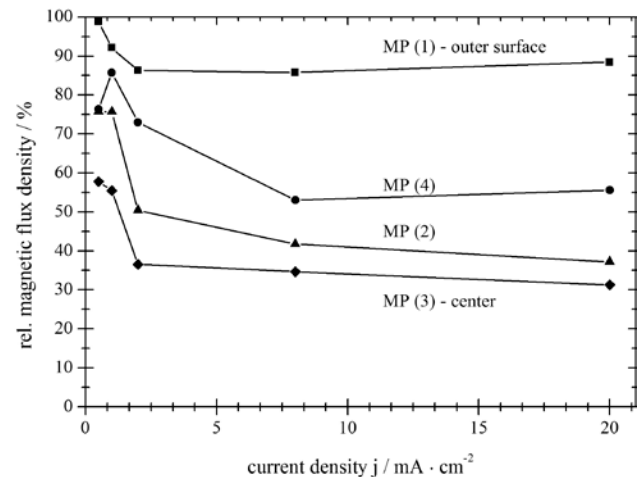

FIG 7 RELATIVE MAGNETIC FLUX DENSITIES OF FOAMS VS. APPLIED CURRENT DENSITY

The relative magnetic flux density has been determined from the field scans as the ratio of the maximal trapped magnetic flux density of each measuring plane and the maximal magnetic flux density of the complete foam which is normally the trapped flux density of the bottom of the foam (MP (5)).

The native foam morphology and structure of the pores is not exactly the same for different foam positions. As a result of this structural inhomogeneity and the statistical distribution of the pores and struts in the foam structure there is a difference in the magnetic flux density of MP (1) and MP (5) although

there should be the same coating thickness. For measuring planes of similar positions, the coating thickness should be the same. The difference in the relative magnetic flux density of the measuring planes (2) and (4) is an artifact of the penetration depth of the Hall probe and hence a consequence of the different measuring volumes (see grey color gradient in Fig. 4). The measuring volume of MP (2) is closer to the foam centre than for MP (4). As a result of the difference in the position of the measuring volumes MP (2) has a lower magnetic flux density than MP (4).

Foams coated with high average current densities show strong inhomogenities in the coating thickness distribution from the outer parts of the foam to the centre. For increasing current densities the relative magnetic flux density of each cut reaches a nearly constant level.

The curve shape of the magnetic flux density for a distinct cut can be explained by the concept of the limiting diffusion current (LDC) of metal ions during the electroplating and indicates a direct proportionality between the magnetic flux density and the LDC of the foam. Each cut has a distinct local LDC. There is a gradient of the metal ions in the electrolyte in the inner of the pores; hence the LDC decreases from regions close to the outer surface to the center of the foam. Based on this concept of local limiting diffusion currents the magnetic flux density is proportional to the coating thickness distribution.

According to these considerations, an increase of the LDC will result in an improvement of the homogeneity of the coating thickness distribution. The LDC can be increased by the use of a more concentrated electrolyte, higher electrolyte temperatures or by an increase of the electrolyte flow through the foam. In this study the LDC has been enhanced by pumping the electrolyte through the foam during the plating process. For a current density of 1 mA/cm² the relative magnetic flux density and the coating thickness, respectively could be increased from 55.5% to 61.3% (in the center of the foam). For a current density of 20 mA/cm² an increase of the magnetic flux density from 31.3% to 44.0% can be found.

The enhancement of the coating thickness homogeneity by an increase of the electrolyte flow intensity is larger than by the reduction of the average current density. This is an evidence that the coating of metal foams via electrodeposition is subjected to very strong mass transport limitations.

Fig. 8 shows the relative magnetic flux densities for different current densities as a function of the position in the foams. For an increase of the current density the curve shape of the magnetic flux density shows more and more an exponential decay.
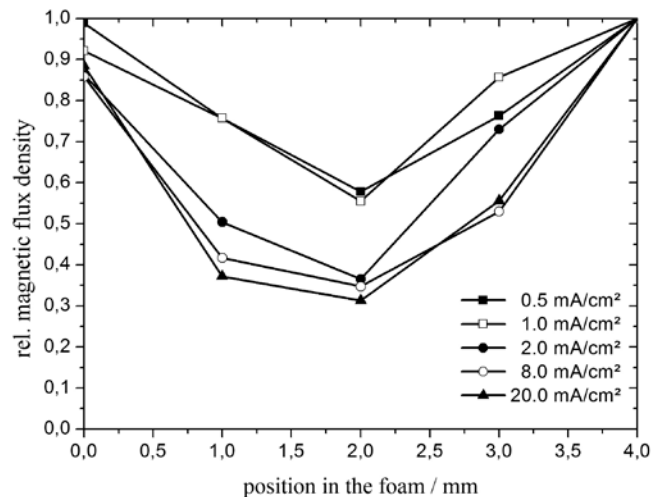

FIG. 8 RELATIVE MAGNETIC FLUX DENSITIES DETERMINED AT DIFFERENT FOAM POSITIONS. THE SAMPLES WERE PREPARED AT DIFFERENT CURRENT DENSITIES

Mass Transport Limitation in Electrodeposition on Metal Foams

To get further information about the mass transport limitations, e.g. the metal ion concentrations during the electrodeposition, cubic 10 ppi foams (50 x 50 x 50 mm³) have been coated with nickel at an average current density of 8 mA/cm² by DC plating (experiment 1), DC with an increased electrolyte flow (pumping the electrolyte) through the foam (experiment 2) and by pulsed electrodeposition (PED) with a duty cycle of 30% and a frequency of 100 Hz (experiment 3). Up to the centre, the foams were cut into rectangular plates with a thickness of 5 mm. The resulting relative magnetic flux densities from the field scans as a function of the position in the coated foam are shown in Fig. 6. The magnetic flux density and hence the thickness of the nickel coating decreases from the outer surface to the center of the foam cube.

For the DC plated foam without pumping the electrolyte through the sample the gradient in the magnetic flux density between two cuts decreases linear to the center of the foam. The measurement ends in a kind of saturation point located near the center of the foam. Based on the direct proportionality between the magnetic flux density and the coating thickness there must be a proportionality to the current density at this position whereas the current

density is proportional to the slope of the ion concentration gradient in the foam. The curve shape of the magnetic flux density distribution for the DC plated foam is in good accordance to the current density distribution in thick porous electrodes made of manganese dioxide or other materials used for batteries [8], [22], [23].

The increase of the flow intensity of the electrolyte through the foam (experiment 2) increases the magnetic flux density of each cut in comparison to the DC plated foam of experiment 1 and hence increase the homogeneity of the coating thickness distribution. The gradient between the first three cuts of the foam of experiment 2 is lower than for the foam of experiment 1. The curve shape becomes more linear.
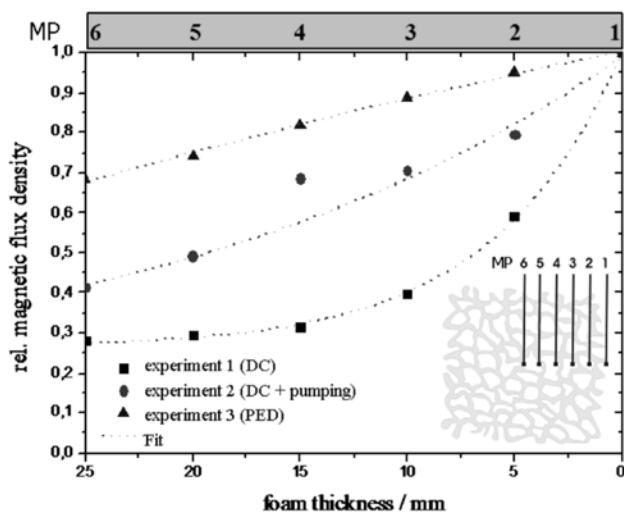

FIG. 9 RELATIVE MAGNETIC FLUX DENSITIES OF A FOAM COATED AT A CURRENT DENSITY OF 8 MA/CM² AS FUNCTION OF THE POSITION IN THE FOAM FOR DIFFERENT PLATING MODES

The foam coated by PED (duty cycle 30%, 100 Hz; experiment 3) has the most homogeneous coating thickness distribution. The coating thickness decreases linearly in direction to the foam center. The flux densities and hence the coating thicknesses for each measuring plane are much higher than for the two DC plated samples. The increase of the magnetic flux density in comparison to the DC plated samples is most distinct for the center of the foam (MP (6)).

Fig. 10 outlines the relative magnetic flux densities of foams coated at different current densities (duty cycle 50%) with and without enhanced hydrodynamics by pumping. As a fact of the lower degree of depletion of ions in the pores by PED higher coating thicknesses in the foam center can be achieved in comparison to DC plating. We find out that an increase of the

hydrodanamics is more important than a decrease of the applied current density. In recent publications concerning the coating of metal foams [6]-[7], an inhomogeneity factor of 2 (ratio of the coating thickness of the outer surface) was found. We could demonstrate that PED (j_m = 2.4 mA/cm²) with the special anode-cathode configuration reduces this factor to 1.25 also for foams with a four-fold thickness. Lower current densities and lower duty cycles with an increased flow of the electrolyte through the foam would let to a further increase of the homogeneity of the coating thickness.
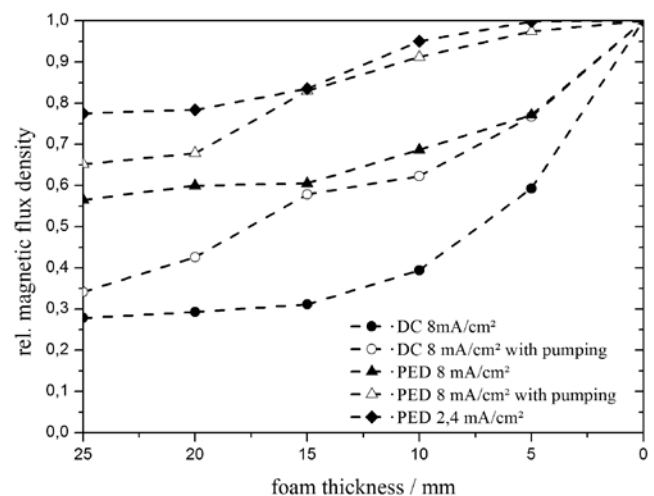

FIG. 10 RELATIVE MAGNETIC FLUX DENSITIES OF A FOAM COATED AT A CURRENT DENSITY OF 8 MA/CM² FOR DC AND PED (DUTY CYCLE 50%) AND PED AT A CURRENT DENSITY OF 2.4 MA/CM² FOR DIFFERENT HYDRODYNAMIC CONDITIONS

Based on these results (see Fig. 9 and 10) it is unavoidable to get a non-uniform coating thickness distribution from experiments without an increased electrolyte flow. In DC plating a very high electrolyte flow is necessary to improve the hydrodynamic conditions that almost uniform coating thickness distributions can be achieved. Also for PED it is not possible to deposit homogeneous coatings without a very strong electrolyte flow. Whereas lower pump intensities should be necessary for PED than for DC plating to implement the same degree of homogeneity. PED causes a more homogeneous coating thickness distribution but is does also changes the properties of the coating and hence the properties of the whole coating-foam composite by influencing the nanostructure. This change in the properties is not ever desirable. The crystallite size is more nanocrystalline and according to the grain boundary strengthening of Hall-Petch [24] the hardness and yield stress of a material are proportional to the reciprocal square root of the crystallite size. Coatings produced

by PED show a higher hardness and stiffness than coatings produced by DC plating. This hardness-increase is associated with a decrease of the coating ductility, hence the coating is more brittle.

A model to describe the mass transport limitation in direct current plating of metal foams on the basis of the above mentioned results is given in Fig. 11.
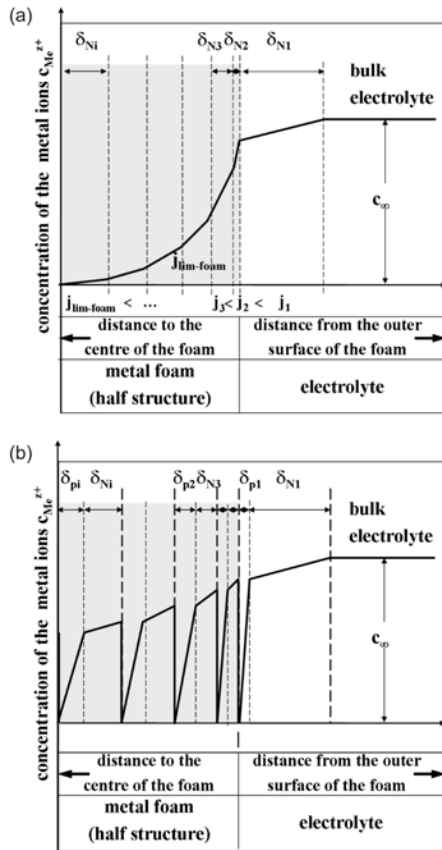

FIG. 11 MASS TRANSPORT LIMITATION MODEL FOR DIRECT CURRENT PLATING (A) AND PULSED ELECTRODEPOSITION (B) OF METAL FOAMS

The model is an extension of the two-dimensional mass transport limitation model for planar electrodes [13] in the third dimension into the foam structure and based on a superposition of Helmholtz layers δ_N with increasing layer thickness in direction to the foam centre. An increasing distance to the bulk electrolyte in direction to the foam center results to a gradual decrease of the concentration gradient between two neighboring Helmholtz layers.

At the outer surface of the foam the metal ions will be spontaneously deposited. This repeats at each Helmholtz layer δ_{Ni} in direction to the foam centre. Based on this large decrease in the ion concentration in the first pore layers the concentration gradient between two neighbouring Helmholtz layers (e.g. δ_{N2}

$\rightarrow \delta_{N3}$) decreases up to the foam centre whereas the layer thickness increases. For each of these Helmholtz layer δ_{Ni} it exists a distinct local LDC j_i which decreases from the first layer δ_{N1} to the last layer δ_{Ni} in the foam centre. The value of theses local LDCs (j_i) depends on the position in the foam. Foam increments can only be coated with nickel in the case that the applied current is less or equal to the local LDC. The LDC of the Helmholtz layer δ_{Ni} is the global limiting diffusion current of the foam $j_{lim\text{-}foam}$. For the same electrolyte the LDC of a theoretical planar electrode with the same side surface is much higher than the global LDC of foams. The local LDCs are in the range between the global LDC of the foam and the corresponding LDC of the theoretical planar electrode. Applying the LDC of a theoretical planar electrode on a foam, it will only be plated at the outer surface - the internal volume remains unplated.

This model is also valid for experiment 2, but the model has to be extended by terms of an increased diffusion or convection in the foam. This causes a reduction of the gradient between two neighboring Nernst layers and hence enlarges the layer thickness.

Due to the current alternation during the t_{on}- and t_{off}-times in PED the model has to be extended by a pulsating diffusion layer δ_{pi}. The concentration of metal ions in this layer pulsates with the pulse frequency between the lowest concentration of the stationary diffusion layer and zero (directly in front of the electrode). The layer thickness of the pulsation diffusion layer decreases with an increasing pulse current density and t_{on}-time and thus with an increase of the duty cycle. Using the same average current density the thickness of the stationary diffusion layer, the Helmholtz layer, remains unchanged. For foams the second diffusion layer is immediately in front of each strut. In the model a pulsating diffusion layer has to be introduced between two Helmholtz layers. During the t_{off}-time there is the relaxation of the concentration of metal ions in the pulsating diffusion layer and thus the depletion of the electrolyte in direction to the center of the foam is diminished.

For direct current plating the shape of the concentration profile in Fig. 11 depends on the pore size, the foam thickness, the hydrodynamic conditions and the average current density. Furthermore in PED the curve shape depends on the duty cycle and the pulse frequency.

It is known that metal foams show an electromagnetic shielding effect [1], [4]. Based on this there could also be

a lowering of the applied current density in direction to the center of the foam by the foam framework itself according to the Faraday shielding effect. This shielding effect interferes with the above mentioned diffusion model. For this reason it is impossible to get a homogeneous coating thickness with a homogeneity factor of 1.0. m

Optimization of the Coating Metal and Coating Thickness by Quasi-static Compression Tests

Fig.12 shows the stress-strain diagrams of nickel and copper based hybride foams, respectively. A coating with copper has no significant positive effect on the mechanical properties, whereas for the nickel coating, there is a linear increase of the plastic collapse stress and the plateau stress but a decrease of the compression and densification point with increasing coating thickness.
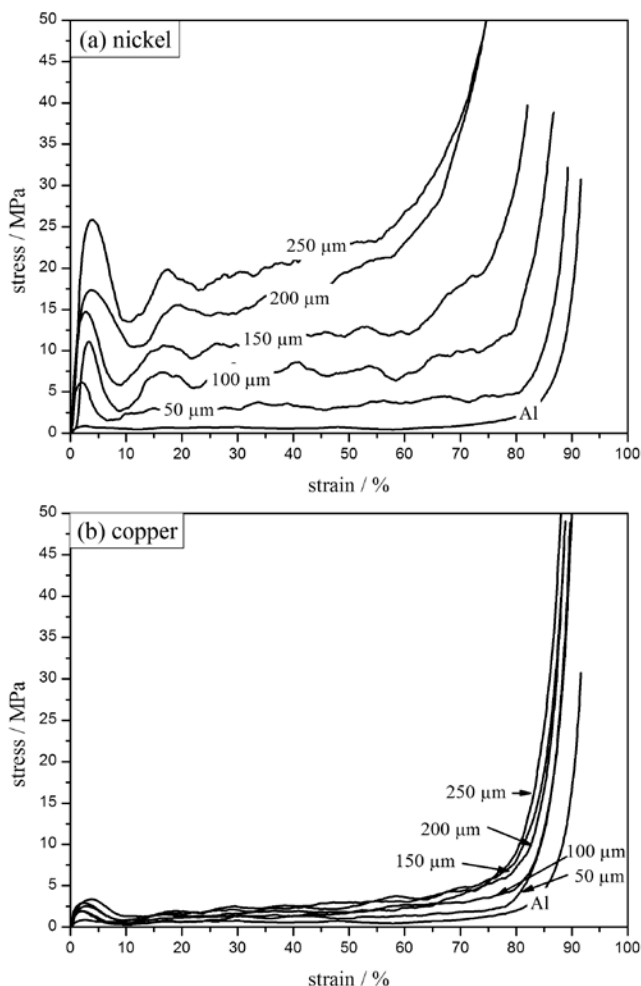

FIG. 12 STRESS-STRAIN DIAGRAMS OF NICKEL (A) AND COPPER (B) HYBRID FOAMS

The energy absorption capacity per foam thickness and per density of both types of hybrid foams is shown in Fig. 13 as function of the coating thickness.

The energy absorption capacity per thickness of the copper hybrid foams shows only a little increase in comparison to the uncoated aluminium foams but due to the larger coating thickness, the increasing mass overcompensates the positive effect of the coating. Hence, there is a halving of the specific energy absorption capacity per density for the hybrid foams in comparison to the aluminium foams. The reason for this behavior is on the one hand the worse mechanical properties of copper in comparison to nickel but principally on the other hand a bad adhesion of the copper coating on the aluminium foam due to corrosion effects during the coating process.
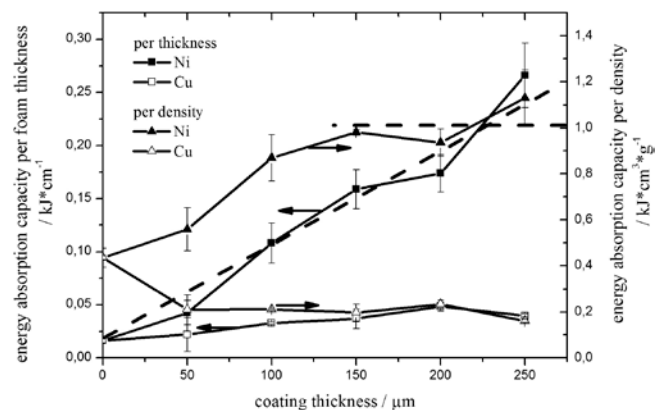

FIG. 13 DEPENDENCY OF THE SPECIFIC ENERGY ABSORPTION CAPACITY OF NICKEL AND COPPER BASED HYBRID FOAMS AS FUNCTION OF THE COATING THICKNESS

For the nickel hybrid foam there is not only a linear increase of the plastic collapse stress and the plateau stress but also of the energy absorption capacity per thickness. Even per density, nickel coated foams improve the energy absorption capacity. First, there is a linear increase with increasing coating thickness. At a coating thickness of about 150 μm nickel the increasing mass compensates the positive effect of the coating. This means, the optimal coating thickness for nickel hybrid foams is 150 μm. For this optimal coating thickness, there is an enhancement of the energy absorption capacity in comparison to the pure aluminium foams by a factor of about 10.

The exact enhancement effects are shown in Table 1.

For a better comparison of the performance of the nickel hybrid foams with the pure aluminium foams the theoretical plastic collapse stress and energy absorption capacity of pure aluminium foams with the same density as the hybrid foams have been calculated according to the model of Gibson and Ashby [25] and

Boonyongmaneerat et al. [7], respectively:

$$\sigma_{pcs} = \sigma_s C \left(\frac{\rho}{\rho_s} \right)^{3/2} \qquad (1)$$

$$U = \sigma_{pl} \left(\varepsilon_d - 0.5\varepsilon_{pl} \right) \qquad (2)$$

Whereas σ_{pl} is the plastic collapse stress of the foam, σ_s is the tensil strength of the aluminium matrix, ρ is the density of foam, ρ_s is the density of the aluminium struts and C is a material constant. U is the energy absorption capacity of the foam, σ_{pl} the plateau stress, ε_d the densification strain and ε_{pl} the flow strain.

TABLE I COMPARISON OF THE MECHANICAL PROPERTIES OF ALUMINIUM FOAMS AND NICKEL HYBRIDE FOAMS WITH THE OPTIMAL COATING THICKNESS. THERE IS A DOUBLING OF THE SPECIFIC ENERGY ABSORPTION CAPACITY PER DENSITY

property	Al foam	nickel hybrid foam 150 μm Ni	enhancement factor
Young's modulus [GPa·kg⁻¹]	6.81	23.74	3.5
plastic collapse stress [MPa·kg⁻¹]	77.13	364.85	4.7
plateau stress [MPa·kg⁻¹]	65.75	252.38	3.8
energy absorption capacity			
per foam thickness [kJ·cm⁻¹]	1.65·10⁻²	15.84·10⁻²	9.6
per density [kJ·cm³·g⁻¹]	0.415	0.978	2.2

Both, the theoretical aluminium foams and the nickel hybrid foams show a disproportional dependency of the plastic collapse stress with increasing density (cf. Fig. 14). According to Thornton [26], this is the proof that bending stresses play an important part during the collapse of the foam structure.

The hybrid foams gain advantage over the theoretical aluminium foams with the same density. This effect results from the increasing bending stiffness of the struts of the foam due to the hard nickel coating. The coating strengthens the outer fiber of the struts where the maximal stress during bending and buckling processes is localized. Depending on the coating thickness the aluminium strut has no portion on the outer fiber and this span completely over the thickness of the nickel coating. Hence, the strength of the strut is mainly governed by the nanocrystalline coating. An increasing coating thickness increases the cross section

of the struts and hence the moment of inertia. The enhancement of the bending stiffness arises from the enhancement of the moment of inertia.
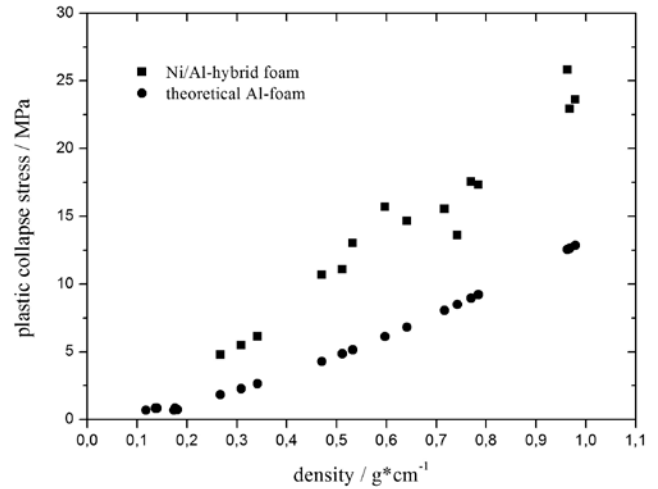

FIG. 14 PLASTIC COLLAPSE STRESS OF NICKEL HYBRID FOAMS AND THEORETICAL ALUMINIUM FOAMS WITH THE SAME DENSITY

The comparison of the energy absorption capacity per density is shown in Fig. 15. Also in this case, the nickel hybrid foams have a much better performance than the theoretical aluminium foams with the same density.
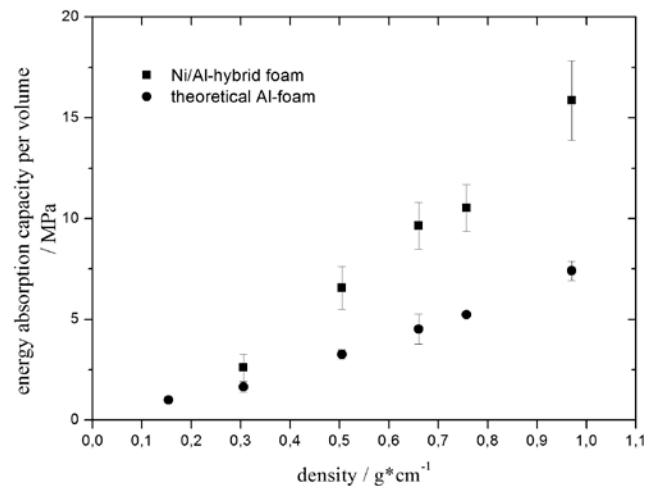

FIG. 15 ENERGY ABSORPTION CAPACITY PER VOLUME OF NICKEL HYBRID FOAMS AND THEORETICAL ALUMINIUM FOAMS WITH THE SAME DENSITY

According to the bending dominated failure mechanism of the pure aluminium foams, there is a quadratic dependency of the energy absorption capacity by the density. The nickel hybrid foams show a linear dependency. This outlines that the predominate failure modes during the plateau phase for the hybrid foams are bending fracture and inelastic buckling. The energy absorption capacity of the

hybrid foams is also strongly affected by the local stress minimum after the plastic collapse stress. This arises from the delamination [6]-[7], [26] of the coating from the substrate foam. A better adhesion between coating and foam reduces the appearance of the local minimum und hence improves the energy absorption capacity [7].

Conclusions

In conclusion we have shown that electrodeposition of metal foams strongly depend on mass transport limitations. The use of field scans of the remanente magnetic flux density was a good method to determine the coating thickness distribution of nickel coated foams and gave important results for the evaluation of a mass transport limitation model in a porous foam electrode during direct current plating or pulsed electrodeposition. In contrast to further attempts in the literature [6]-[7] we could demonstrate that a more homogeneous coating thickness distribution for thicker foams can be achieved by using a special cage like anode, an enhanced hydrodynamic electrolyte flow, and the use of low current densities combined with low duty cycles. The mismatch ratio of the coating thickness of the outer struts of the foam and the centre could be reduced of 1.25. As a fact of the electromagnetic shielding of the outer ligaments of the foams it will not be possible to produce foams with a totally homogeneous coating thickness distribution over the complete cross section of thick foams. Further work in this field should be done with different duty cycles to evaluate a more detailed mass transport limitation model with respect to detailed parameter identification.

In quasi-static compression tests, we were able to show the significant increased performance of the nickel hybrid foams not only in comparison to the uncoated aluminium foam substrates but also to theoretical pure aluminium foams having the same density as the hybrid foams. The compression strength and load-bearing capacity, respectively of the hybrid foams arise solely from the coating that forms a network of interconnected, nanocrystalline tubes. But the improvement of the energy absorption capacity results from a complex interaction between the substrate foam structure and the mechanical properties of the nanocrystalline shell.

REFERENCES

[1] M.F. Ashby, A. Evans, N.A. Fleck, L.J. Gibson, J.W. Hutchinson and H.N.G. Wadley, *Metal Foams: a Design Guide*, Butterworth-Heinemann, Woburn, USA, 2000; p. 1-5.

[2] M. Barrabés, A. Michiardi, C. Aparicio, P. Sevilla, J.A. Planell and F.J. Gil, "Oxidized Nickel-Titanium Foams for Bone Reconstructions: Chemical and Mechanical Characterization", *J. Mater. Sci: Mater. Med.* 18, pp. 2123-2129, 2007.

[3] J. Banhart, J. Baumeister, and M. Weber, "Offenporige Aluminiumschäume – Eigenschaften und Anwendungen", *Aluminum*, 75(12), pp. 209, 1994.

[4] J. Banhart, "Manufacturing, Characterization and Application of Cellular Metals and Metal Foams", *Prog. Mater. Sci.*, 46(6), pp. 559-632, 2001.

[5] M.D. Demetriou, J.S Harmon, W.L. Johnson, and C. Veazey, "Amorphous Metal Foams as a Property-matched Bone Scaffold Substitute", WO/ patent 2008/021358, Feb. 21, 2008.

[6] B. Bouwhuis, J. McCrea, G. Palumba and G. Hibbard, "Mechanical Properties of Hybrid Nanocrystalline Metal Foams", *Acta Mater.*, 57(14), pp. 4046-4053, 2009.

[7] Y.C. Boonyongmaneerat, C. Schuh and D. Dunand, "Mechanical Properties of Reticulated Aluminium Foams with Electrodeposited Ni-W Coatings", *Scripta Mater.*, 59(3), pp. 336-339, 2008.

[8] K.J. Euler, "Stromverteilung in und auf Porösen Elektroden", *Chemie-Ing.-Techn..*, 37(6), pp. 626-631, 1965.

[9] A. Jung, H. Natter, S. Diebels, E. Lach, R. Hempelmann, "Nanonickel Coated Aluminum Foam for Enhanced Impact Energy Absorption", *J. Adv. Eng. Mater.*, 13, pp. 23-28, 2011.

[10] H. Natter, M. Schmelzer and R. Hempelmann, "Nanocrystalline Nickel and Nickel-Copper Alloys: Synthesis, Charcterization, and Thermal Stability", *J. Mater. Res.*, 13, pp. 1186-1197, 1998.

[11] H. Natter and R. Hempelmann, "Tailor-made Nanomaterials Designed by Electrochemical Methods", *Electrochim. Acta*, 49, pp. 51-61, 2003.

[12] A. Jung, H. Natter, R. Hempelmann and E. Lach, "Nanocrystalline Alumina Dispersed in Nanocrystalline Nickel: Enhanced Mechanical Properties", *J. Mat. Sci.*, 44, pp. 2725-2735, 2009.

[13] C.H. Hamann and W. Vielstich, *Elektrochemie*, Weinheim, Wiley-VCH, 2005; p 191.

[14] R.C. Sisk and A.J. Helton, "Scanning Instrumentation for Measuring Magnetic Field Trapping in High T_c Superconductures", *J. Rev. Sci. Instrum.*, 64, pp. 2601-2603, 1993.

[15] W. Xing, B. Heinrich, H. Zhou, A.A. Fife and A.R. Cragg, "Magnetic-Flux Mapping, Magnetization, and Current Distribution of $YBa_2Cu_3O_7$ Thin-Films by Scanning Hall Probe Measurements", *J. Appl. Phys.*, 76, pp. 4244-4255, 1994.

[16] D.A. Cardwell, M. Murakami, M. Zeisberger, W. Gawalek, R. Gonzalez-Arrabal, M. Eisterer, H.W. Weber, G. Fuchs, G. Krabbes, A. Leenders, H.C. Freyhardt, X. Chaud, R. Tournier and N. Hari Babu, "Round Robin Measurements of the Flux Trappping Properties of Melt Processed Sm-Ba-Cu-O Bulk Superconductors", *Physica C*, 412, pp. 623-632, 2004.

[17] C. Christides, I. Panagiotopoulos, D. Niarchos and G. Jones, , *Sensors and Actuators A*, 106, pp. 243-245, 2003.

[18] A. Jung, H. Natter, R. Hempelmann, S. Diebels, M.R. Koblischka, U. Hartmann and E. Lach, "Study of the Magnetic Flux Density Distribution of Nickel Coated Aluminium foams", *J. Phys.: Conf. Series*, 200, pp. 1-4, 2011. (http://iopscience.iop.org/1742-6596/200/8/ 082011).

[19] B.E. Warren and L.E. Averbach, "The Effect of Cold-Work Distortion on X-Ray Patterns", *J. Appl. Phys.*, 21, 595-599, 1950.

[20] D.J. Balzar, "X-Ray Diffraction Line Broadening – Modelling and Applications to High-T_c Superconductors", *J. Res. Nat. Inst. Stand. Technol.*, 98, pp. 321-353, 1993.

[21] H. Natter and R. Hempelmann, "Nanocrystalline Copper by Pulsed Electrodeposition: The Effects of Organic Additives, Bath Temperature, and pH", *J. Phys. Chem.*, 100 (50), pp. 19525-19532, 1996.

[22] K. Fischbeck and E. Einecke, *Z. Anorg. Allg. Chem.*, 148, pp. 97, 1925.

[23] J.J. Coleman, *Trans. Electrochem. Soc.*, 90, pp. 545, 1951.

[24] E.O. Hall, "The Deformation and Aging of Mild Steel. 3. Discussion of results", *Proc. Phys. Soc. London B*, 64, 747-753, 1951.

[25] L.J. Gibson and M.F. Ashby, *Cellular solids*, 2nd ed., Cambridge University Press, 1997.

[26] P. Thornton and C. Magee, "Deformation of Aluminium Foams", *Metall. Trans. A*, 6(6), pp. 1253-1263, 1975.